Plasma Physics Reports, Vol. 30, No. 8, 2004, pp. 671–686. Translated from Fizika Plazmy, Vol. 30, No. 8, 2004, pp. 722–738.

PLASMA KINETICS

Nonequilibrium Electron Distribution Functions in a Semiconductor Plasma Irradiated with Fast Ions

S. I. Kononenko[1], V. M. Balebanov[2], V. P. Zhurenko[1], O. V. Kalantar'yan[1], V. I. Karas'[3], V. T. Kolesnik[1], V. I. Muratov[1], V. E. Novikov[4], I. F. Potapenko[5], and R. Z. Sagdeev[6]

[1] *Kharkov National University, pl. Svobody 4, Kharkov, 61077 Ukraine*

[2] *Institute for Space Research, Russian Academy of Sciences, Profsoyuznaya ul. 84/32, Moscow, 117810 Russia*

[3] *National Science Center, Kharkov Institute for Physics and Technology, ul. Akademicheskaya 1, Kharkov, 61108 Ukraine*

[4] *Science and Technology Center of Electrophysical Treatment, National Academy of Sciences of Ukraine, Kharkov, Ukraine*

[5] *Keldysh Institute of Applied Mathematics, Russian Academy of Sciences, Miusskaya pl. 4, Moscow, 125047 Russia*

[6] *University of Maryland, College Park, MD, USA*

Received October 21, 2003

Abstract—A kinetic equation for the electrons scattered by acoustic phonons in a solid is derived, and relationships between power-law asymptotic solutions and the particle and energy fluxes in phase space are established. The dependence of the nonextensivity parameter on the intensity of the particle flow in phase space is determined for a nonequilibrium solid-state plasma with sources and sinks. The formation of a steady-state nonequilibrium electron distribution function in a semiconductor with a source and a sink in phase space is numerically simulated using the Landau and Fokker–Planck collision integrals. The nonequilibrium electron distributions formed in the solid-state plasmas of semiconductors and of a Sb/Cs cathode are studied experimentally. It is shown that, within the electron energy range of 5–100 eV, the electron distribution functions decrease with energy according to a power law. © *2004 MAIK "Nauka/Interperiodica".*

1. INTRODUCTION

At present, the development of high-power particle and radiation sources is stimulating great interest in the properties of nonequilibrium systems. The presence of sources and sinks in momentum space can lead to the formation of nonequilibrium particle distribution functions with power-law tails even in spatially uniform systems. The inapplicability of the local equilibrium approximation to such situations is related to the presence of particle flows in phase space. In the second section of this paper, the asymptotic properties of such nonequilibrium states are studied, their relation to the nonextensive Tsallis' thermodynamics is established, and the dependence of the nonextensivity parameter on the intensity of the particle flow in phase space (i.e., on the intensities of sources and sinks) is determined.

The third section is devoted to numerical simulations of the formation of a steady-state nonequilibrium distribution of particles with a long-range repulsion potential. The collisional dynamics of such a system is studied using spatially uniform nonlinear Landau and Fokker–Planck collision integrals, which are model representations of the Boltzmann collision integral. In numerical simulations, completely conservative difference schemes are used.

In the fourth section, we consider the conduction and emission properties of a semiconductor plasma irradiated with intense particle or laser beams.

In the fifth section, the formation of nonequilibrium electron distribution functions (EDFs) in the plasmas of semiconductors and of a Sb/CS cathode is studied experimentally. To study these functions, the method of the secondary electron emission induced by fast low-Z ions was employed. The formed EDFs are measured, the coefficients of the secondary ion-induced electron emission are determined, and their relationship to the source power in the ion's track is found.

2. STEADY NONEQUILIBRIUM STATES OF SYSTEMS WITH STATIONARY PARTICLE FLOWS IN PHASE SPACE

Quasi-steady nonequilibrium states of particle systems can be studied by solving kinetic equations with allowance for sources and sinks. Power-law particle energy distributions were first predicted theoretically in [1–4] and then observed experimentally in [5, 6]. In [1, 2], it was shown using a similarity transformation that the kinetic Boltzmann equation for a spatially uniform system has exact stationary power-law solutions. In [3, 4], it was shown by directly calculating the Boltzmann and Landau collision integrals in kinetic equations that the power-law distributions of the form

$$F(E) = AE^{-s}, \tag{1}$$

where s is an exponent and A is a constant, are stationary solutions for which particle (or energy) fluxes in

1063-780X/04/3008-0671$26.00 © 2004 MAIK "Nauka/Interperiodica"

phase space are nonzero constants. These particle states are similar to turbulent Kolmogorov spectra of waves and depend only on the integral characteristics of the source and sink [4].

In particular, nonequilibrium spatially uniform systems with a component obeying a power-law distribution include electron subsystems of semiconductors exposed to radiation with a photon energy on the order of the width of the forbidden zone [7] or electron subsystems in metals that undergo ionization caused by α particles propagating in them [5].

In [1–4], the exponent s of power-law solutions to the kinetic Boltzmann equation depended only on the degree of homogeneity of the particle interaction potential. In those papers, both the dispersion properties of a plasma with a power-law electron distribution and the ionization equilibrium in such nonequilibrium steady states were studied. In [8, 9], it was shown that plasma oscillations with a linear dispersion can exist in a plasma with two components of the distribution function, equilibrium and nonequilibrium. These plasma oscillations could be of importance for many interactions in semiconductor plasma, in particular, for the plasmon mechanism of superconductivity [10].

2.1. Basic Equations

It is of interest to examine the cases in which the effect of a source on the deviation of the distribution function from equilibrium can be clearly traced.

Exact solutions to the Boltzmann equation for a spatially uniform gas were first obtained in [11] within a special collisional model (a gas of Maxwellian molecules) for the relaxation to a thermodynamic equilibrium. The generalization to a nonequilibrium case was performed in [12]. Note that the method described in [11] was generalized to a wide class of power-law intermolecular potentials [13].

One can construct mathematical models for the collision integral in kinetic equations so that these equations, on one hand, become more appropriate for analysis and, on the other hand, still possess some of their important properties inherent to complete nonlinear equations, such as conservation laws and the H theorem [11, 14].

In this paper, we investigate the features of steady-state nonequilibrium particle distributions in systems with sources and sinks by the example of the interactions of electrons with phonons in a solid-state plasma. Main attention is paid to the evolution of such states with changes in the parameters of nonequilibrium (particle fluxes) in a system, rather than their time evolution.

To describe electron kinetics, we use a spatially uniform nonlinear (because of the incorporation of quantum statistics) kinetic equation with sources and sinks [15]:

$$\frac{\partial f}{\partial t} = -\frac{1}{4\pi v^2}\frac{\partial}{\partial v}\Pi\{f, v\} + \Psi(v). \quad (2)$$

In the case of an isotropic medium, it is convenient to change the variables: $\varepsilon = v^2/2$ and $F(\varepsilon) = 4\pi\sqrt{2\varepsilon}\,f(\sqrt{2\varepsilon})$, where v is the particle velocity normalized to the mean particle velocity v_{0T} in the initial state.

Let us consider an important class of sources that are localized in energy space, $S_+(\varepsilon) = Q_i\varepsilon_i\delta(\varepsilon - \varepsilon_i)$. The sinks are often written in the form $S_-(\varepsilon) = \nu(\varepsilon)F(\varepsilon)$. Using these model representations, the expression describing the sources and sinks can be written as

$$\Psi(\varepsilon) = S_+(\varepsilon) - S_-(\varepsilon). \quad (3)$$

For charged particles interacting with phonons, the expression for the particle flux in the kinetic equation takes a simple form,

$$\Pi(\{f\}, v) = D(v)\frac{\partial f}{\partial v} + F(v)f(v)(1 - f(v)), \quad (4)$$

where the diffusion coefficient $D(v)$ and the drag force $F(v)$ for a particle moving in phase space are power-law functions of the electron energy (the corresponding expressions for some particular cases are given in [16]). Within the region where the flux P is constant, the equation for the steady-state distribution function (for the above type of interaction) is

$$T_0\frac{\partial f}{\partial \varepsilon} + f - f^2 = \frac{P}{\varepsilon^2}, \quad (5)$$

where $T_0(\varepsilon) = \dfrac{D(\varepsilon)}{F(\varepsilon)}$. After substituting $f(\varepsilon) = -\dfrac{T_0}{y(\varepsilon)}\dfrac{dy(\varepsilon)}{d\varepsilon}$, this equation converts into the second-order linear equation

$$T_0^2\frac{d^2y(\varepsilon)}{d\varepsilon^2} + T_0\frac{dy(\varepsilon)}{d\varepsilon} + \frac{P}{\varepsilon^2}y(\varepsilon) = 0. \quad (6)$$

2.2. Solutions to Eq. (6)

A general solution to Eq. (6) is

$$y(\varepsilon) = C_1 I_\chi\left(\frac{\varepsilon}{2T_0}\right) + C_2 K_\chi\left(\frac{\varepsilon}{2T_0}\right), \quad \chi = \sqrt{\frac{1}{4} - \frac{P}{T_0^2}}, \quad (7)$$

where $I_\chi(z)$ and $K_\chi(z)$ are the modified Bessel function of the first and second kinds, respectively. The integration constants are determined from the matching condition for solution (7) and the equilibrium solution in the regions beyond the inertial interval.

To clarify the effect of the degree to which the system is nonequilibrium (the source intensity) on the shape of the EDF in a solid, we present the results from the numerical solution of the kinetic equation for several P values.

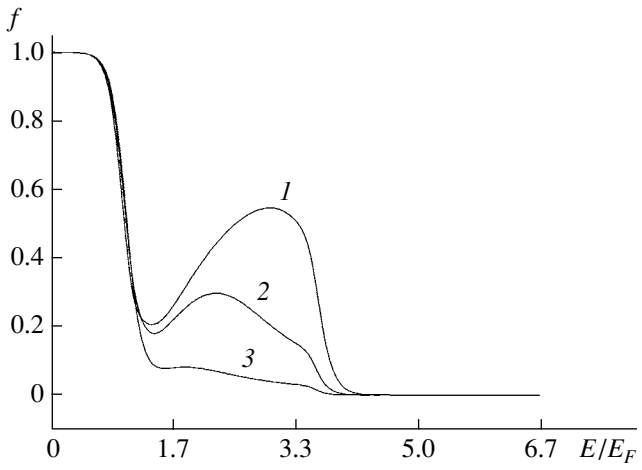

Fig. 1. Distribution functions of the electrons scattered by acoustic phonons at $T = 0.1E_F$ for P = (*1*) –0.81, (*2*) –0.4, and (*3*) –0.1.

The solutions to the kinetic equation for the case of electron scattering by the phonons with a temperature of $T_0 = 0.1E_F$ (where E_F is the Fermi energy) are shown in Fig. 1. It can be seen that the nonequilibrium part of the distribution function increases with source intensity.

The time evolution of the EDF is illustrated in Figs. 2–4. Figures 2 and 3 show how the distribution function and the particle flux in phase space relax to their steady-state values in the presence of sources and sinks. It can be seen from Fig. 3 that phase space regions with a quasi-constant energy flux eventually form. It follows from Figs. 3 and 4 that, in the region where the flux is constant, quasi-power-law zones arise in the distribution function. The regions with zero flux (see Figs. 2, 4) correspond to the equilibrium Fermi function.

In the region where the EDF is nonequilibrium, it is well approximated by power-law functions with an exponent that varies only slightly with increasing source intensity. This is clearly seen in Fig. 4, which shows a steady-state EDF between the source and sink on a double logarithmic scale.

2.3. Tsallis' Nonextensive Thermodynamics

As was mentioned above, steady-state nonequilibrium distributions (SND) of particles in phase space play the same role in spatially uniform systems as Maxwellian distributions in Gibbs' thermodynamics. The presence of such great deviations from the exponential dependence should significantly change the thermodynamic properties of a system.

Note that, over the last fifteen years, great progress has been achieved in the thermodynamics of strongly nonequilibrium systems; the results obtained indicate the existence of non-Gibbs (power-law) distributions in such systems. Let us briefly outline the results that will be needed further for our analysis.

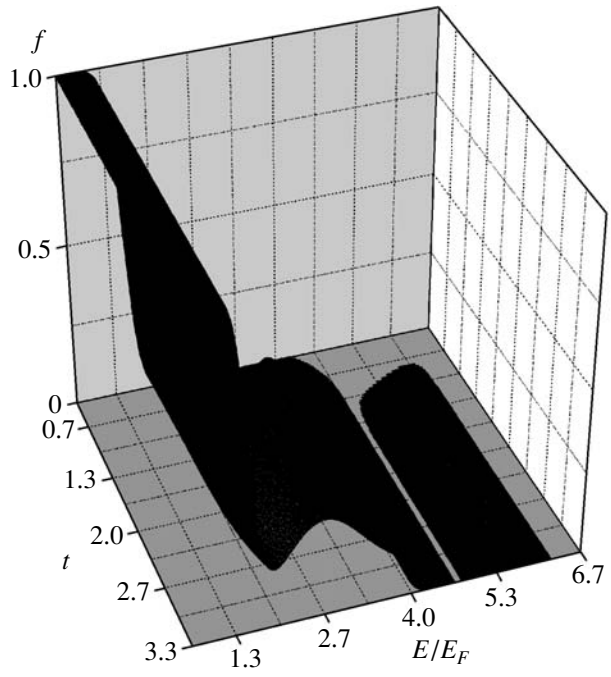

Fig. 2. Distribution function as a function of time and energy for P = –0.4.

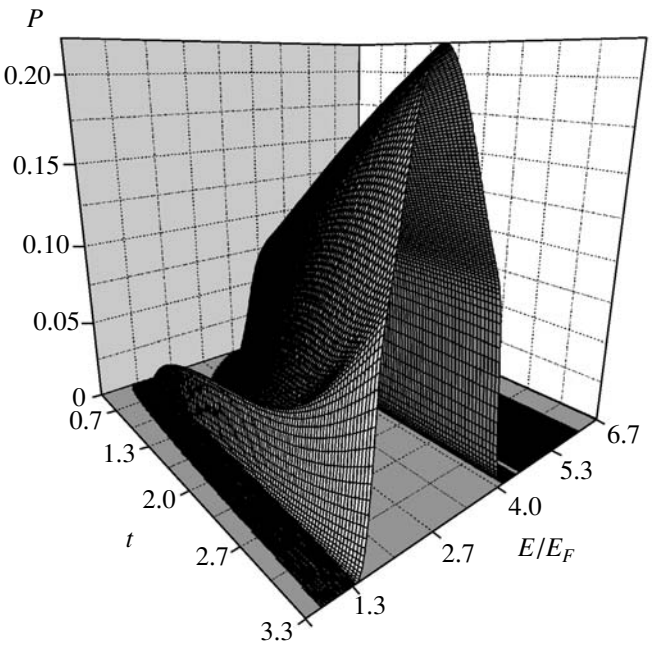

Fig. 3. Particle flux in phase space as a function of time and electron energy for P = –0.4.

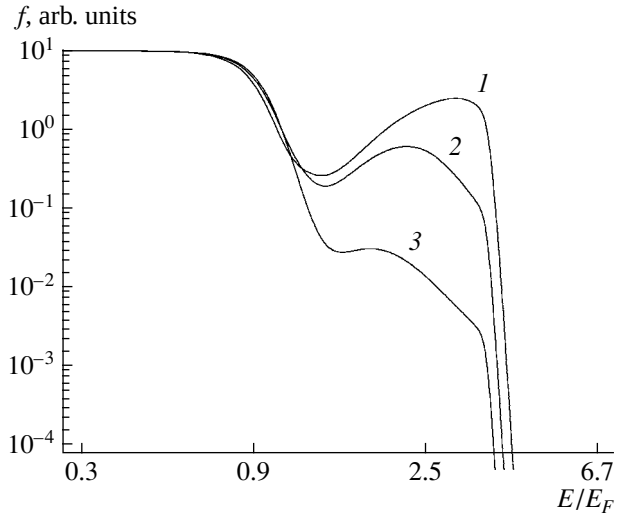

Fig. 4. Distribution functions for $P = (1) -0.81$, $(2) -0.4$, and $(3) -0.1$.

In 1988, K. Tsallis [17] attempted to extend the applicability range of thermodynamics and statistic mechanics to systems in which entropy does not possess the property of extensivity [17].

It is well known that, in conventional thermodynamics, the equilibrium state corresponds to the maximum possible entropy at a given energy, volume, etc. In addition, it is assumed that entropy is an extensive quantity. This assumption immediately leads to some important consequences.

Let us recall the definition of an extensive quantity. Let the system consists of two *independent* subsystems *A* and *B*. Entropy is an extensive quantity if the entropy of the entire system is equal to the sum of the subsystem entropies:

$$S(A + B) = S(A) + S(B).$$

In statistical physics, entropy is treated via the number of system microstates. In trying to define entropy so that it is an extensive quantity, statistical physics has to invoke a hypothesis of molecular chaos. This hypothesis assumes that, *before a collision*, any colliding molecules be definitely uncorrelated, i.e., not affecting one another. For many (but not for all) systems, this is a quite reasonable assumption. It is from this assumption that the Boltzmann expression for the entropy of a closed system follows:

$$S = -\sum_i p_i \ln(p_i),$$

where i is the number of the system microstate, p_i is the probability that the system is in this microstate, and the summation is performed over all microstates.

After [17], a great number of systems were studied in which the extensivity of entropy and the Boltzmann thermodynamics were violated. Examples of such systems are a cold interstellar dust cloud of sufficiently large size and a system of colliding high-energy hadrons whose interaction is characterized by strong correlations. There are other systems that cannot be described by Boltzmann thermodynamics. The reasons why Boltzmann thermodynamics is inapplicable are quite different [17]. These could be "memory effects," due to which the current state of the system depends not only on the values of the system parameters at a given instant but also on the values they had some time ago.

Memory effects can easily violate the hypothesis of molecular chaos. These effects imply that, before a collision, individual particles "remember" one another, so that their motion is not completely uncorrelated. Hence, thermodynamic relations must be refined with allowance for additional correlations. An attempt at such a refinement was made by Tsallis [17]. In his thermodynamics, the logarithmic and exponential functions in the conventional expressions for entropy and distribution function were formally replaced with expressions containing power-law functions:

$$\ln(x) \longrightarrow \ln_q(x) = \frac{x^{1-q} - 1}{1 - q},$$

$$\exp(x) \longrightarrow \exp_q(x) = (1 + (1 - q)x)^{1/(1-q)}$$

with a certain numerical parameter q. Note that, as q tends to unity, $\ln_q(x)$ and $\exp_q(x)$ transform into the ordinary logarithmic and exponential functions (this can easily be checked, e.g., by their differentiation). A new formula for entropy is

$$S_q = -\sum_i p_i^q \ln_q(p_i) = \frac{1 - \sum_i p_i^q}{q - 1}. \qquad (8)$$

As $q \longrightarrow 1$, the q-entropy converts into the conventional Boltzmann entropy.

The main consequence of such a substitution is that q-entropy is no longer an extensive function. When the system is divided into two independent subsystems, *A* and *B*, we obtain

$$S_q(A + B) = S_q(A) + S_q(B) + (1 - q)S_q(A)S_q(B).$$

Thus, the parameter q is a measure of system nonextensivity. We note that, generally, the parameter q is not in any way limited and can take any value from $-\infty$ to $+\infty$; certain restrictions can, however, be imposed in solving one or another specific problem.

In [18], it was shown that the condition for the q-entropy to be at maximum leads to power-law functions

$$p(E) = \exp_q(-(E/T)). \qquad (9)$$

The above functional form of the q-entropy was chosen rather arbitrarily, and its main importance is as a model description of nonextensivity.

Thus, there is a set of different thermodynamics. Indeed, for $q = 1$, the above general approach results in conventional thermodynamics. If q is not equal to unity, then the physical situation is qualitatively different from equilibrium thermodynamics.

2.4. Features of the Electron Kinetics in Semiconductor Plasma at Energies Higher than the Fermi Energy

In studying the relaxation of high-energy electrons in semiconductor plasma, it is best to use a kinetic equation in the form of a nonlinear Fokker–Planck equation with a Landau collision integral. Below, we use dimensionless variables: the velocity is in units of the thermal velocity and time in units of the electron–electron relaxation time τ_{ee}, which, in the case of Coulomb interaction, is equal to $\tau_{ee} = \dfrac{v_T^3 m^2}{4\pi n_p e^4 \ln\Lambda}$, where $\ln\Lambda$ is the Coulomb logarithm. The dimensionless EDF $f(v, t)$ is normalized so that $n_p = \int_0^\infty f(v, t) v^2 dv = 1$ and $E = \int_0^\infty f(v, t) v^4 dv = \dfrac{3}{2} T = 1$, where T is the electron temperature in energy units.

At high source intensities, the relaxation of the particle flow between collisions should be taken into account. For this reason, it is necessary to move from the conventional representation of the Fokker–Planck equation in the form of a parabolic equation to a set of equations of hyperbolic type:

$$\frac{\partial f}{\partial t} = I_{nlFP}[f, f] + \Psi(v),$$

$$I_{nlFP}[f, f] = -\frac{1}{4\pi v^2}\frac{\partial}{\partial v} J_{nl}\{f, v\}, \qquad (10)$$

$$\tau\frac{\partial J_{nl}}{\partial t} + J_{nl} = \Pi_{nl}(v, \{f(v)\}).$$

To simplify analysis, we reduce the expression for the particle flux to a symmetric form [23],

$$\Pi_{nl}(v, \{f(v)\}) = -\frac{4\pi}{v}\frac{\partial}{\partial v}\int_0^v f(v)P(x) - f(x)P(v)]x^2 dx, \qquad (11)$$

$$P(v) = 2\int_v^\infty f(x) x dx.$$

The calculation of flux (12) in velocity space for a power-law EDF described by Eqs. (10) yields the following expression:

$$\Pi(v, q) = A\Big(C_{22}F_1\Big(\frac{3}{2}, \frac{1}{q-1}; \frac{5}{2}; -(q-1)v^2\Big) - 3\Big(5C_1 - C_2\exp_q(v^2)_2F_1\Big(\frac{5}{2}, \frac{1}{q-1}; \frac{7}{2}; -(q-1)v^2\Big)\Big)\Big), \qquad (12)$$

with the constants

$$C_1 = v^{\frac{2}{q-1}} + 2(q-1)v^{\frac{2q}{q-1}} + (q-1)^2 v^{2+\frac{2q}{q-1}} - \Big(\frac{1}{q-1}\Big)^{\frac{1-2q}{q-1}}\Big(1 + \frac{1}{(q-1)v^2}\Big)^{\frac{1}{1-q}} \times\Big(\Big((q-1)^{-\frac{q}{q-1}} + (q-1)^{-\frac{1}{q-1}}v^2\Big)\Big)^2,$$

$$A = \frac{(q-1)^2 v^{\frac{q-3}{q-1}}(1 + (q-1)v^2)^{\frac{1+q}{1-q}}\Gamma\Big(\frac{1}{q-1}\Big)\Gamma\Big(\frac{2-q}{q-1}\Big)}{15\pi^3\Gamma^2\Big(\frac{5-3q}{2q-2}\Big)}, \qquad (13)$$

$$C_2 = 2(q-1)v^{2+\frac{2q}{q-1}}\exp_q(v^2).$$

This function, which represents a surface in (v, q) space, is shown in Fig. 5. The steady-state states correspond to regions in which the flux does not depend on velocity. Two such regions are seen in Fig. 5. The first is the region with $q = 1$, which corresponds to an equilibrium Maxwellian solution, while the second corresponds to states with power-law asymptotes obtained in [3–5].

The hyperbolic character of the set of equations allows one to efficiently use the method of straight lines to numerically analyze the system evolution. The dependence of the EDF on velocity (or energy) is represented by its values at discrete points. The time evolution of the EDF values at these points can easily be described by the set of nonlinear ordinary differential (over time) equations.

Note that, in the case of quantum statistics, the formal generalization of an equilibrium Maxwell–Gibbs distribution function with the use of function (12) to nonequilibrium states is ambiguous. Indeed, an equilib-

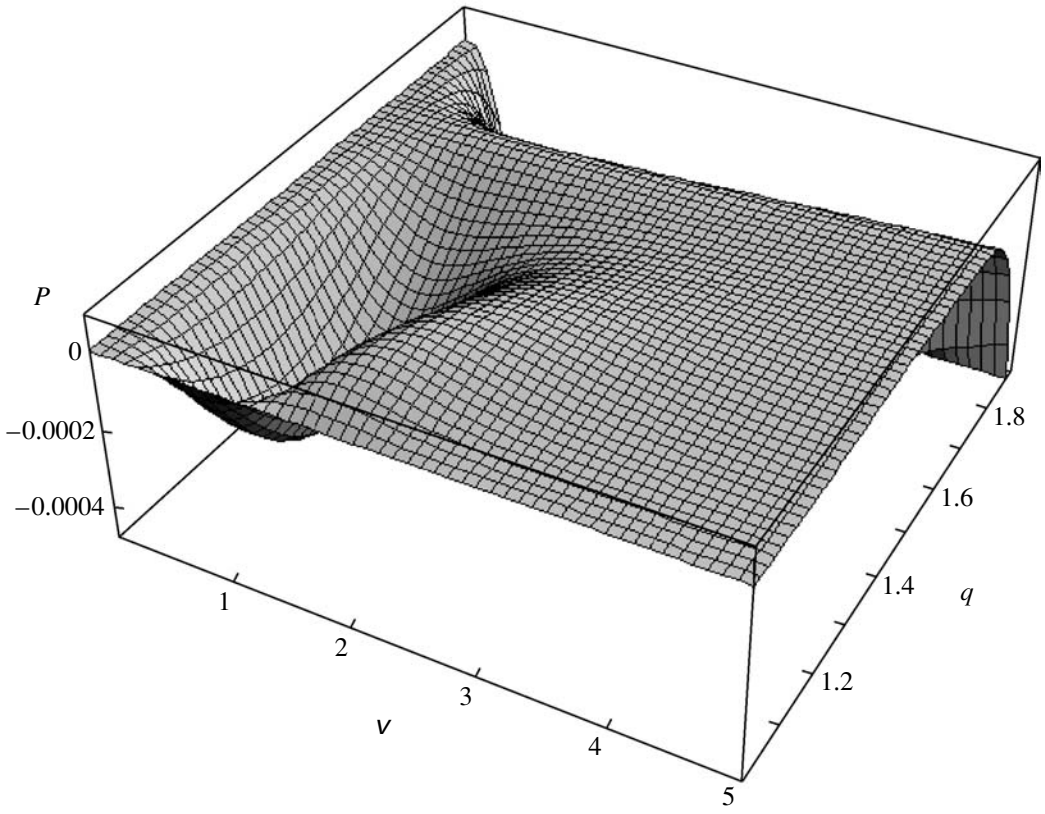

Fig. 5. Particle flux in phase space vs. velocity and nonextensivity parameter q.

rium Fermi function can be represented in two equivalent forms:

$$f(\varepsilon) = \frac{1}{1 + \exp\left(\frac{\varepsilon - E_F}{T}\right)}$$
$$= \frac{\exp\left(-\frac{\varepsilon - E_F}{2T}\right)}{\exp\left(\frac{\varepsilon - E_F}{2T}\right) + \exp\left(-\frac{\varepsilon - E_F}{2T}\right)}. \quad (14)$$

Substituting function $\exp_q(x)$ for the exponential function in these expressions, we obtain two nonequivalent generalizations to nonequilibrium states for a Fermi function. At $q \longrightarrow 1$, both these functions convert into a Fermi distribution function. However, when deviating from equilibrium, variations in the distribution function

$$f_q(\varepsilon) = \frac{\exp_q\left(-\frac{\varepsilon - E_F}{2T}\right)}{\exp_q\left(\frac{\varepsilon - E_F}{2T}\right) + \exp_q\left(-\frac{\varepsilon - E_F}{2T}\right)} \quad (15)$$

occur mainly in the region near the Fermi energy, while the second function

$$f_q(\varepsilon) = \frac{1}{1 + \exp_q\left(\frac{\varepsilon - E_F}{T}\right)} \quad (16)$$

acquires a power-law asymptote at high energies. One can prove that distribution function (15) is a good approximation for the EDF formed in the interactions with phonons, while distribution function (16) adequately describes steady-state nonequilibrium solutions to a kinetic equation with a Landau collision integral with allowance for corrections related to the Fermi statistics.

So far, we have considered the formation of an SND with sources and sinks localized in momentum space. It should be noted that one often has to deal with systems in which both the source and the sink are nonlocalized. In particular, wake ionization is a source that is not localized in momentum (energy) space. Moreover, the source intensity is often insufficient to provide a universal nonequilibrium distribution throughout the interval between the source and sink (see [19, 20]). In these cases, it is necessary to resort to numerical simulations.

3. NUMERICAL SIMULATIONS OF THE FORMATION OF STEADY-STATE NONEQUILIBRIUM PARTICLE DISTRIBUTIONS

A specific feature of systems of particles interacting via the Coulomb potential is that the scattering cross section increases without bound as the momentum transferred tends to zero. For gaseous and semiconductor plasmas with a large Coulomb logarithm ($\ln\Lambda = 10$–15), one can restrict oneself to the expansion of the integrand in the collision integral in small momenta transferred (a diffusion approximation) and to represent the collision integral in the Landau or Fokker–Planck form [21, 22], which are model representations of the Boltzmann collision integral. In this model [23–25], the moments of the exact and model collision integrals coincide up to the third-order tensor moment and the forth-order scalar moment. Conservation laws for energy and the number of particles, as well as the Boltzmann *H* theorem, are valid. The model collision integral provides a correct representation of the equations for the twenty-moment Grad approximation. Finally, the exact solution to the Landau equation for Maxwellian molecules ($\beta = 4$) is the exact solution to the Boltzmann equation. Below, we will consider long-range potentials ($U \propto r^{-\beta}$, with $1 \le \beta \le 4$, where r is the distance between the interacting particles), for which a local nonequilibrium particle distribution can form (see [3]). Note that the dynamics of particles interacting via the Coulomb repulsion potential ($\beta = 1$) can be considered using kinetic equations in either the Landau or Fokker–Planck form.

3.1. Formulation of the Problem

In the case of an isotropic distribution function $f(v, t)$, the Landau collision integral is

$$\frac{\partial f}{\partial t} = I_L[f, f] = \frac{\Gamma}{v^2}\frac{\partial}{\partial v}\left\{\frac{1}{v}\int_0^\infty dw Q(v, w) \times\left[wf(w)\frac{\partial f(v)}{\partial v} - vf(v)\frac{\partial f(w)}{dw}\right]\right\}, \quad (17)$$

$$Q(v, w) = \frac{a(v, w)(v + w)^{\eta+4} + b(v, w)|v - w|^{\eta+4}}{(\eta + 2)(\eta + 6)},$$

$$0 \le v, \quad w < \infty, \quad t \ge 0,$$

$$a(v, w) = [vw - (v^2 + w^2)],$$

$$b(v, w) = [vw + (v^2 + w^2)], \quad \eta = (\beta - 4)/\beta,$$

where $\Gamma = 4\pi e^4(\ln\Lambda)/m$ and the symmetric kernel $Q(v, w) = Q(w, v)$ in the case of Coulomb potential has the form $Q(v, w) = -2/3w^3$ for $w \le v$ and $Q(v, w) = -2/3v^3$ for $w \ge v$. The equilibrium solution to Eq. (17) is a Maxwellian distribution function

$$f_{\text{Maxw}} = n\frac{4}{\sqrt{\pi}}v_T^{-3},$$

where $v_T = \sqrt{2k_B/m}$, k_B is the Boltzmann constant, and T is temperature. If there are no sinks (sources), then the number of particles and the system energy do not vary over time:

$$n_p = \int_0^\infty f(v, t)v^2 dv = \text{const},$$

$$E = \int_0^\infty f(v, t)v^4 dv = \frac{3}{2}k_B T = \text{const}.$$

The distribution function $f(v, t)$ is bounded at $v = 0$ and quite rapidly decreases as $t \longrightarrow \infty$. Below, we use dimensionless variables: the velocity in units of the thermal velocity $V_T = \sqrt{3/2}v_T$ and time in units of the electron–electron relaxation time τ_{ee}, which is $\tau_{ee} = \frac{v_T^3 m^2}{4\pi n_p e^4 \ln\Lambda}$ in the case of Coulomb interaction. The function $f(v, t)$ is normalized so that $n_p = 1$, $E = 1$ and $v_T^2 = 2/3$; consequently, in Eq. (17), the constant Γ is equal to unity.

Note that, when numerically simulating a low-density collisional plasma ($\beta = 1$) under laboratory conditions or for astrophysical applications, the Fokker–Planck collision integral

$$\frac{\partial f}{\partial t} = I_{FP}[f, f] = \frac{1}{v^2}\frac{\partial}{\partial v}\left[A(v)\frac{\partial f}{\partial v} + B(v)f(v, t)\right],$$

$$0 \le v < \infty, \quad t \ge 0,$$

is commonly used in the kinetic equation. For numerical simulations, it is most suitable to represent the Fokker–Planck equation in symmetric form (11).

We consider the formation of a steady-state nonequilibrium solution in the presence of particle or energy flows in velocity space using the above modified versions of the Landau and Fokker–Planck collision integrals in forms (17) and (11), respectively. In this case, the right-hand side of the kinetic equation is added with the terms accounting for the presence of a particle (energy) source (sink):

$$\frac{\partial f}{\partial t} = I_{FP, L}[f, f] + S_+ - S_-. \quad (18)$$

The source (sink) function was modeled by an exponential function with a variable width in momentum

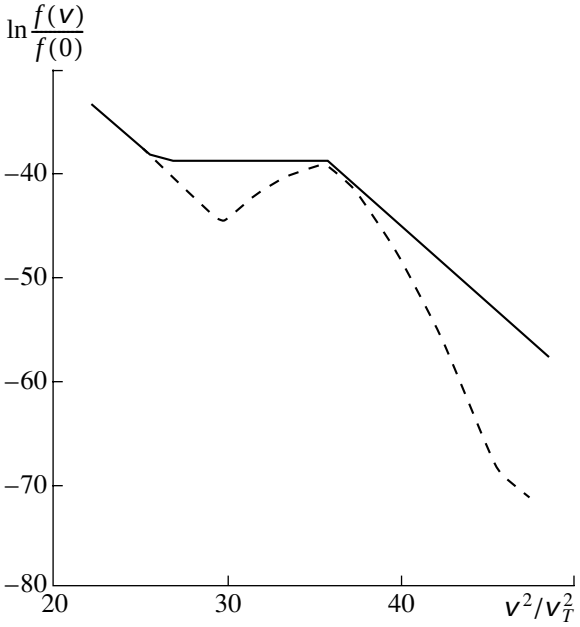

Fig. 6. Distribution functions obtained from the Fokker–Planck equation with a source and a sink of the form $S_\pm \sim I_\pm \exp\{-\alpha_1(v - v_\pm)^2\}$ with $\alpha_1 = 100$, $v_- = 4$, and $v_+ = 7$. The dashed and solid curves refer to the times $t = 25$ and 100, respectively.

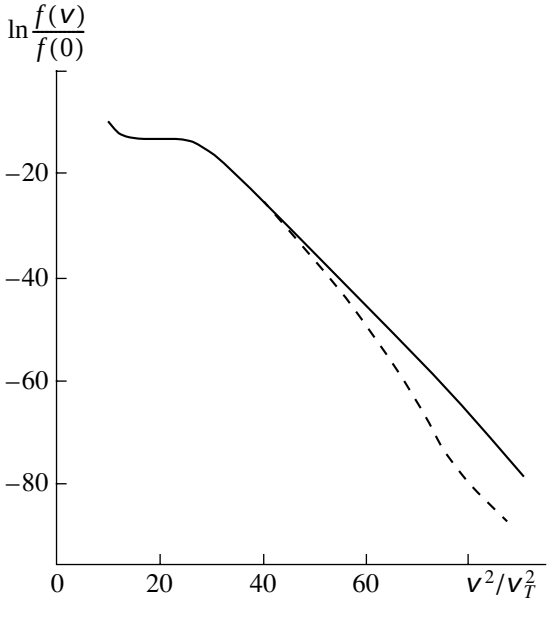

Fig. 7. Distribution functions obtained from the Fokker–Planck equation with a source and a sink of the form $S_\pm \sim I_\pm \exp\{-\alpha_1(v - v_\pm)^2\}$ with $\alpha_1 = 10$, $v_- = 3$, and $v_+ = 5$. The dashed and solid curves refer to the times $t = 25$ and 100, respectively.

space, $S_\pm \sim I_\pm \exp\{-\alpha_1(v - v_\pm)^2\}$; a δ function in the form $S_\pm \sim I_\pm \delta(v - v_\pm)/v^2$; or

$$S_\pm \sim I_\pm \frac{\delta(v - v_\pm)}{v^2} f(v_-, t). \qquad (19)$$

In this case, if $I_+ = I_-$, then an energy flow from the source to sink arises; if $I_+ = I_- \frac{v_-^2}{v_+^2}$, then a particle flow arises. The flow direction is determined by the positions of v_- and v_+. Either a Maxwellian distribution or a δ function was used as an initial distribution. In simulations, we employed a fully conservative implicit difference scheme [23–25], for which discrete analogues of conservation laws hold true and which allow one to perform long-run calculations without error accumulation. An infinite velocity interval was replaced with the maximum interval $10v_T$–$14v_T$, in which the distribution function was set at zero. The initial distribution $\delta(v - v_0)$ was approximated in the following way: the δ function was set at zero for all of the velocities except for one point (usually, $v_0 = 1$).

Since the problem of relaxation is a kind of test, we first consider the Cauchy problem for the initial distribution $f^0(v) = \delta(v - 1)/v^2$. In our calculations, we used the kinetic equation with either the Fokker–Planck or Landau collision integral in form (11) or (17), respectively. When $S_\pm = 0$, these equations are analytically equivalent and, in the limit $t \longrightarrow \infty$, lead to a Maxwellian distribution f_{Maxw}. Let us now discuss the results of numerical simulations.

3.2. Discussion of the Simulation Results

In [23], the formation of a nonequilibrium distribution function was numerically simulated for the kinetic equation with either the Landau or Fokker–Planck collision integral in the presence of energy and particle flows in momentum space that were sustained by a source and a sink. For this purpose, the right-hand sides of kinetic equations (17) and (11) were supplemented with various types of sources S_+ and sinks S_-. First, solutions were obtained for the case where the positions of a source and a sink in momentum space were matched with the direction of a flow sustained by collisions. Note that analytic consideration of equations for the case of a localized source and sink gives a correct flow direction, namely, from high to low velocities [3]. It was shown in [23] that, within the interval between the source and sink, an SND (of the Kolmogorov kind) of particles is established with time. This distribution corresponds to the presence of an energy flow in momentum space, whereas beyond this interval, the distribution function is thermodynamically equilibrium. When using the Landau equation, the particle distribution relaxes to an SND by more than one order of magnitude faster than when the Fokker–Planck equation is used. As was noted above, the positions of the

source and sink and the direction of flow in momentum space should be matched with one another. To make sure once again that this requirement is important, we performed calculations with the interchanged positions of the source and sink in energy space. It turned out that variations in the flow intensity by several orders of magnitude did not influence the equilibrium particle distribution when the source and sink positions were not matched with the flow direction.

The dependence of the EDF on the degree of the source and sink localization in energy space is illustrated in Figs. 6 and 7. It can seen that the behavior of the SND in most of the interval between the source and sink does not depend on the degree of the source (sink) localization; this indicates the local (universal) character of the solution.

Figure 8 shows the distribution functions for different flow intensities. It is found that, for low intensities of the source I_+ (sink I_-), a universal nonequilibrium distribution is formed in the velocity range $v \le v_+$. This is due to (i) a decrease in the cross section for Coulomb scattering with increasing velocity ($\sim v^{-3}$) and (ii) the ever-present flow of energy and particles (due to Coulomb diffusion) toward the region of the main ("background") equilibrium distribution. Consequently, as the source (sink) intensity increases, a universal nonequilibrium particle distribution is formed that occupies a progressively larger space between the source and sink. Such behavior is related to a decrease in the fraction of the flow transferred to the background plasma. It is worth noting that the increase in intensity is accompanied by an increase in the magnitude of the nonequilibrium distribution function in proportion to the flux magnitude [3].

Let us examine the form of the distribution function for power-law interaction potentials with the exponents $1 \le \beta \le 4$. Note that $\beta = 1$ corresponds to the Coulomb interaction potential, $\beta = 2$ corresponds to dipole interaction, and $\beta = 4$ describes the interaction of so-called Maxwellian molecules. Figure 9 shows nonequilibrium distribution functions for the case of a steady-state energy flow with an intensity of $I = 0.01$ and $\beta = 1$, 2, and 4. It can be seen that, for all these β values, the exponents of the formed nonequilibrium power-law distribution functions are close to one another, which agrees with the results of [3]. The magnitude of the nonequilibrium part of distribution function decreases with increasing β. These results are in qualitative agreement with the above analytic predictions.

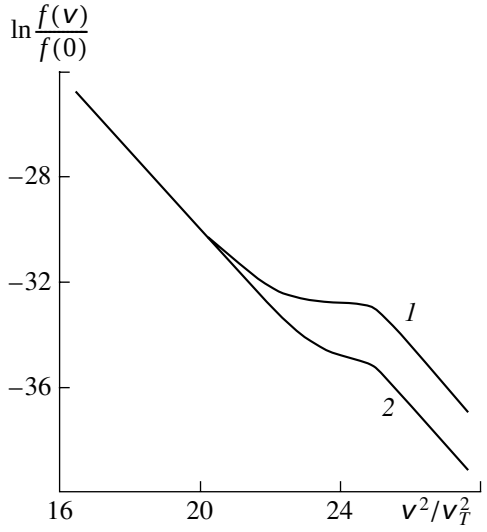

Fig. 8. Steady-state distribution function obtained from the Landau equation for $\beta = 1$ and an exponential source sink and sink at two values of the flux intensity in phase space: $I_1 = 0.01$ and $I_2 = 0.001$ ($v_- = 4$, $v_+ = 5$).

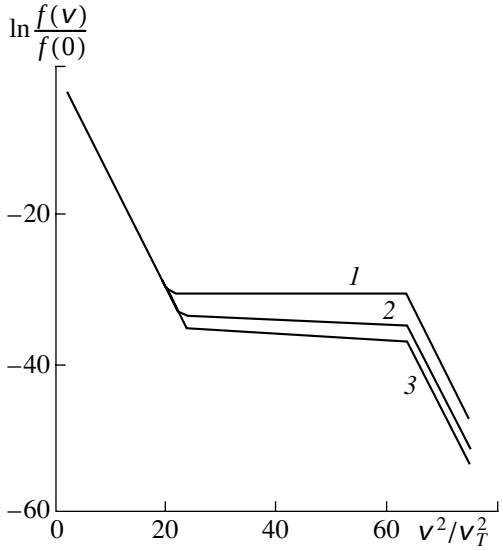

Fig. 9. Steady-state nonequilibrium distribution functions vs. squared velocity for a constant energy flux with an intensity of $I = 0.01$. The source and sink are in the form of δ function (19) with $v_- = 4$ and $v_+ = 8$. Curves *1*, *2*, and *3* are calculated using the collision integrals in the Landau form with exponents $\beta = 1$, 2, and 4, respectively.

4. FORMATION OF THE EDF IN THE INTERACTION OF RADIATION AND PARTICLE BEAMS WITH SOLID-STATE PLASMA

In this section, we consider the conduction and emission properties of a semiconductor plasma irradiated with intense particle or laser beams.

A comparison of the characteristic times of ionization and relaxation shows that, in the case at hand, the steady-state EDF should be determined mainly by electron–electron collisions [3]. Hence, it can be obtained from the condition that the Boltzmann collision integral (for a semiconductor plasma, the Landau or Fokker–Planck collision integral) be zero.

It follows from the above analysis that, for a semiconductor plasma in the energy range $E - E_F > E_F$, a power-law distribution with a nonzero flux of energy or particles in momentum space can be established. This distribution is formed due both to collisions with electrons whose energy is in the range $E - E_F > E_F$ and background (equilibrium) electrons.

It was shown above that a nonequilibrium electron distribution is close to a universal distribution if the intensity of the flow produced by the source and sink in momentum space is sufficiently high.

Let us consider, as an example, the irradiation of a solid-state plasma with a beam of fast ions (with velocities higher than the velocities of atomic electrons) or high-power electromagnetic radiation with the frequency ω satisfying the condition $\hbar\omega \gg k_B T$. In both these cases, a great number of high-energy electrons arise that, in accordance with the above consideration, form a nonequilibrium steady-state EDF. When the distribution function is nonequilibrium, the emission current density is anomalously high since the distribution function decreases very slowly over the inertial interval. The plasma conductivity is determined by the density of current carriers. In the case of a nonequilibrium EDF, the carrier density in semiconductor plasma is very high in comparison to the case of an exponentially decreasing equilibrium EDF. Therefore, when a semiconductor plasma is irradiated with intense radiation or particle beams, an anomaly in the emission and conduction properties of plasma should be observed. Indeed, such an anomaly was observed, e.g., in [26, 27].

Supplying additional kinetic energy to a solid-state plasma results in the ionization of atoms and the production of a rather large number of free electrons with energies higher than the equilibrium (thermal) energy [28]. Under these conditions, nonequilibrium distributions of free electrons can form [3, 4]. It was shown in a series of theoretical and experimental studies that, when a solid-state plasma is irradiated with fast ion beams, a steady-state nonequilibrium power-law EDF

$$f(E) = \alpha I^{1/2} E^{-s} \tag{20}$$

is formed in the plasma due to the presence of a particle (energy) flow produced by a source (ionization) and a sink (electron emission) in momentum space. In Eq. (20), α is the normalizing factor, I is the particle (energy) flux, s is an exponent [4, 5], and E is the total electron energy in a solid ($E = \varphi + E_F + eU$, where φ is the work function and eU is the energy relative to the electron energy in vacuum). Power-law distributions are characterized by a rather large fraction of high-energy electrons. For example, when a Be sample is irradiated with 4.9-MeV α particles, the fraction of electrons with energies higher than $E_p = 18.9$ eV (where E_p is the energy of plasma eigenmodes in beryllium) can exceed 37% [29].

When the velocity v of an incident ion is much higher than the velocities of the target's electrons, the elastic losses are negligibly small, whereas the inelastic energy losses, which are usually called ionization loss, are described by the Bethe–Bloch formula [30]

$$-dE/dx = (4\pi Z_1^2 e^4/mv^2) Z_2 N \ln(2mv^2/I), \tag{21}$$

where m is the electron mass; Z_1 is the charge number of the incident ions; Z_2 is the atomic number of the target material; and N and I are the density and the average excitation potential of the target's atoms, respectively. It follows from formula (21) that, at high energies, the ionization loss decreases as v^{-2}. The introduction of an extra charge in a quasineutral equilibrium solid-state plasma leads to the displacement of free electrons with respect to their equilibrium positions and to the excitation of plasma eigenmodes (plasmons) [31]. Thus, the energy lost by an ion due to its deceleration is transferred to the target's electrons in two ways: a certain fraction of the energy is spent on the excitation of plasmons, while the rest energy is transferred to individual electrons in collisions (in particular, in collisions with atoms, which then become ionized) [28]. Such a nonequilibrium external action significantly changes the distribution function of free electrons [4].

A fraction of the nonequilibrium electrons that have proper magnitudes and momentum directions can escape from the target; i.e., these electrons can take part in the process of secondary ion-induced electron emission (SIEE). The emission proceeds in three stages:

(i) origin of nonequilibrium electrons,

(ii) their collisions and motion (diffusion) toward the surface of a solid, and

(iii) overcoming the potential barrier by these electrons and their escape into vacuum.

Such an approach is believed to most comprehensively account for the SIEE features and has been widely used since the Sternglass study [32] (see also [33]). The processes of electron diffusion to the surface and overcoming the potential barrier seem to be the same for the electrons produced by ion bombardment and the electrons produced as a result of target irradiation by electron or laser beams [34].

An integral characteristic of SIEE is the SIEE coefficient γ, often called the electron yield (see [35]). The electron yield γ is defined as the ratio of the number of knocked-out secondary electrons N_e to the number of incident ions N_i,

$$\gamma = N_e/N_i. \tag{22}$$

The SIEE coefficient depends substantially on the energy of incident ions. It has been shown both theoretically and experimentally that, for low-Z ions, the electron yield γ is proportional to the average specific ionization loss of ion energy in matter, dE/dx [32, 35, 36].

A much more informative characteristic of SIEE is the electron energy distribution. It has been shown experimentally that the energy spectra of secondary electrons are of power-law character [6, 37, 38]. When

studying electron emission from some metals, it was shown that the distribution functions of the electrons knocked out by low-Z ions are piecewise power-law functions with different exponents s for different energy ranges [5, 6, 39].

As was shown in [40], emissivity variations accompanying the irradiation of a sample with intense charged particle beams can be efficiently used to create new energy sources. One such source is a secondary-emission radioisotope current source [41] that converts the energy of α particles into electrical energy using the nonequilibrium properties of the electron distributions. Since the efficiency of this source is proportional to the difference between the electron yields of the employed emitter materials ($\gamma_2 - \gamma_1$) [41], it is necessary to use an emitter with the maximum possible γ_2 value to increase the source efficiency.

At present, the available literature data on the emission properties of materials irradiated with fast ion beams mainly refer to metals. Note that no data are available in the literature on the efficient electron emitters widely used in the photoemission and electronic techniques. Among the most widely used efficient emitters of secondary electrons are emitters based on Sb/Cs compounds. Due to the large coefficients of secondary electron emission (SEE) and photoemission (this is usually related to the low potential barrier at the boundary between the sample surface and vacuum), such compounds have been widely used in manufacturing the photocathodes and dynodes in photomultipliers and other devices [42]. To illustrate, the SEE coefficient σ for Sb/Cs compounds is 3–4 at low energies of primary electrons ($E_e \sim 100$ eV) and reaches its maximum value of $\sigma_{max} = 8$–10 at $E_e = 500$–600 eV [42]. Such large SEE coefficients are presumably explained not only by the low work function for this material but also the formation of a power-law nonequilibrium distribution function.

5. EXPERIMENT

This section is devoted to our experimental studies aimed at revealing the main features of the EDFs formed during the irradiation of a Sb/Cs cathode and certain semiconductors with a beam of fast low-Z ions.

5.1. Experimental Setup

A schematic of the experimental setup used to study the EDFs formed in the solid-state plasmas of semiconductors and of a Sb/Cs cathode irradiated with a beam of fast low-Z ions is shown in Fig. 10.

An electrostatic Van de Graaf generator used as a source of primary particles provided beams of H^+ or He^+ ions. Energy spectra of SIEE electrons were measured for H^+ beams with ion energies from 1.00 to 2.25 MeV and He^+ beams with ion energies from 1.75 to 2.25 MeV. The ion energy was varied with a step of

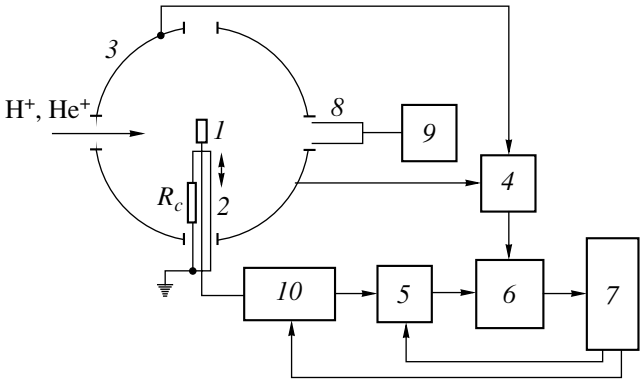

Fig. 10. Schematic of the experimental setup: (*1*) target, (*2*) target holder, (*3*) hemispheres, (*4*, *5*), electrometric amplifiers, (*6*) analog-to-digital converter, (*7*) PC, (*8*) Faraday cup, (*9*) F303 current meter, and (*10*) saw-tooth voltage generator.

0.25 MeV. The cathode used as a target was a Sb/Cs layer deposited on a massive nickel substrate. The layer thickness was less than the mean free path of the incident ions in Sb/Cs. A 10-mm-diameter target (*1*) fixed in a copper mount was installed on a movable holder (*2*). The ion beam collimated by a system of diaphragms was incident onto the target and caused SIEE from its surface. The target plane was normal to the beam axis. The beam diameter on the target surface was 3 mm, and the ion current density was no higher than 30 $\mu A/cm^2$. The chamber was evacuated with an NMD-0.4-1 magnetic-discharge pump and an NVPR-16D backing pump with a liquid nitrogen trap. In all our experiments, the residual gas pressure in the vacuum chamber was no higher than 10^{-6} torr.

The electrons emitted from the target surface were intercepted by a spherical collector consisting of two 100-mm-radius hemispheres (*3*). The target and the holder were set inside the collector. The gap between the hemispheres was 15 mm. The diameter of the entrance window of the hemisphere was 10 mm. Besides the collector current, we also measured the target current I_T, which was the sum of the beam ion current I_B and the current of the secondary electrons that reached the collector: $I_T = |I_C| + I_B$. The measured I_C and I_T currents amplified by electrometric amplifiers (*4* and *5*, respectively) were applied to a PC (*7*) through an analog-to-digital converter (*6*). To calibrate the measurement system, a Faraday cup (*8*) was set behind the rear hemisphere. The Faraday cup allowed us to directly measure the ion beam current I_{FC} when the target was removed from the beam path. The diameter and length of the Faraday cup were 20 and 130 mm, respectively. The current from the Faraday cup I_{FC} was measured with an F303 current meter (*9*). The SIEE coefficient was determined by the formula

$$\gamma = |I_C|/(I_T - |I_C|). \quad (23)$$

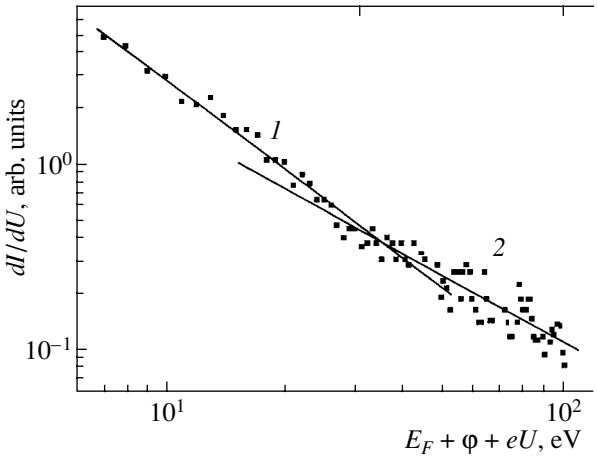

Fig. 11. Typical dependence of $\log(dI/dU)$ on $\log(E_F + \varphi + eU)$, plotted on a double logarithmic scale, for a Sb/Cs cathode bombarded with 1.75-MeV He^+ ions. Energy ranges *1* (5–30 eV) and *2* (30–100 eV) correspond to the exponents $s_1 = 2.9$ and $s_2 = 2.5$, respectively.

By measuring the energy spectrum of SIEE electrons with a spherical analyzer and assuming that emission is produced by a point source, one can reconstruct the EDF inside the target [20]. When the EDF is power-law function (20), the derivative of the emission current with respect to the electron energy, dI/dU, can be written as

$$dI/dU = B(E_F + \varphi + eU)^{-s+1}, \qquad (24)$$

where B is a constant. Hence, on a logarithmic scale, dependence (24) is a straight line with a slope equal to $-s + 1$.

The energy distributions of the secondary emission electrons were measured with a spherical collector operating in the energy-analyzer regime with a retarding field varied in the range 0–100 V with a step of 1 V. The retarding electric potential was applied between the target (*1*) and two hemispheres (*3*). Since the radius of the energy analyzer significantly exceeded the target size, the field distribution was close to spherical. A 5-mm-diameter ceramic tube with an outer surface covered with a resistive layer served as a target holder (*2*). The specific resistance of the layer R_c was varied nonlinearly along the tube so that the holder potential did not disturb the field inside the energy analyzer. One end of the resistive layer was in contact with the target, whereas its other end was grounded. The retarding potential was applied to the target from a saw-tooth generator (*10*) controlled by a PC (*7*). Thus, the current flowing along the resistive layer produced the needed potential distribution along the holder. In experiments, the secondary electrons moved along radial trajectories and reached the collector. When the retarding voltage was applied to the target, only the electrons whose energy was high enough to get through the retarding field reached the collector. The computer software for controlling the experiment allowed the gathering of a 7-s-long time sample consisting of 100 measurements of the electron emission current for each value of the retarding field. These 100 experimental points were then averaged, and the resultant value of the electron current was stored in the PC memory. By differentiating the measured dependence of the collector current on the retarding voltage (the so-called retarding curves), one can deduce the energy spectrum of SIEE electrons and then reconstruct the EDF.

Table 1

Ion	Energy, MeV	Exponent	
		s_1	s_2
H^+	1.25	2.9	2.5
	1.50	3.0	2.5
	1.75	2.9	2.5
	2.00	3.0	2.4
	2.26	3.0	2.6
He^+	1.75	2.9	2.5
	2.00	2.8	2.2
	2.26	2.8	2.3

The exponents s of power-law EDFs were evaluated as follows. First, the time samples of the electron emission current were processed and the delay curves were differentiated. Then, the dependences of dI/dU on the total electron energy $E_F + \varphi + eU$ in the compound under study, plotted on a logarithmic scale, were approximated by straight lines. According to formula (24), the slopes of these straight lines are equal to $-s + 1$.

5.2. Experimental Results and Discussion

The measurements of the energy spectrum of SIEE electrons show that, over the entire ion energy range under study, the nonequilibrium EDF formed in the plasma of a Sb/Cs cathode is a power-law function.

A typical nonequilibrium EDF obtained for a sample bombarded with 1.75-MeV He^+ ions is shown in Fig. 11. The experimental points are quite well fit by two straight lines corresponding to two different exponents, s_1 and s_2, in the energy ranges of 5–30 eV and 30–100 eV, respectively. These exponents for the two parts of the EDF in the above energy ranges are shown in Table 1 as functions of the energy of the incident H^+ and He^+ ions.

In our opinion, the exponent of a power-law distribution function of secondary electrons could depend on the energy (specific ionization loss) of fast ions. It seems that it is the specific ionization loss that determines the intensity of the source of extra particles in momentum space. It was shown in [4, 43] that, under certain conditions, the exponent is independent of the structure of the source and sink. In this case, it can be said to be a universal power-law distribution function with an exponent equal to –5/4 [43]. In our previous experiments with a He^+ beam and thin metal films, in which the exponents s were measured, it was shown that the absolute value of the exponent s_1 of a power-law distribution function in the first energy range corresponding to slow electrons ($E < 35$ eV) decreases with increasing specific ionization loss of ions in a substance [39]. In [38], it was pointed out that the fraction of fast electron increases with increasing energy of the incident ions. It can be seen from Table 1 that the exponents s_1 for different incident ions and, accordingly, different specific ionization losses in a Sb/Cs sample differ insignificantly, although, for protons, the exponent increases with ion energy and decreases with specific ionization loss. No such dependence was observed for helium ions. It should be noted that variations in the exponent do not exceed 10%; to deduce the exact dependence of the exponent on the energy loss requires additional study.

Figure 12 shows the dependence of the electron yield γ on the energy of the incident H^+ and He^+ ions for a Sb/Cs cathode. It can be seen that, for the Sb/Cs compound under study, the electron yield γ exceeds that for some metals [35]. The reason could be as follows. As was mentioned above, a fraction of the nonequilibrium electrons produced in a solid-state plasma under bombardment with a beam of fast charged particles diffuse toward the surface and escape into vacuum. Electron emission proceeds from the surface layer, whose thickness is much less than the depth to which the ions penetrate into the target and is determined by the features of the electron motion toward the surface. In metals, the generated electrons, while diffusing toward the surface, interact mainly with conduction electrons. This interaction may proceed via pair collisions and collective effects—the excitation of plasmons. Due to the large density of conduction electrons in metals, the probability of electron–electron interactions and, accordingly, the effective escape depth of secondary electrons are small. In semiconductors, the density of conduction electrons is low; hence, the escape depth of secondary electrons can be quite large. Since Sb/Cs compounds possess semiconductor properties [42], the escape depth of nonequilibrium electrons can be larger than in metals. The higher (compared to metals) value of the SIEE coefficient can be, to a certain extent, explained by this factor.

Sb/Cs compounds have low work functions [44]. The relatively low potential barrier at the boundary between such a compound and vacuum may lead to an increase in the fraction of nonequilibrium electrons leaving the solid. The work function determines the cutoff energy for the nonequilibrium power-law EDF formed in a solid-state plasma. Since the exponent within the first energy interval is fairly high (see Table 1 and [6, 37–39]), even a slight decrease in the work function leads to a significant increase in the SIEE coefficient.

Our experiments have shown that, for all of the energies of H^+ and He^+ ions, the EDFs formed in a semicon-

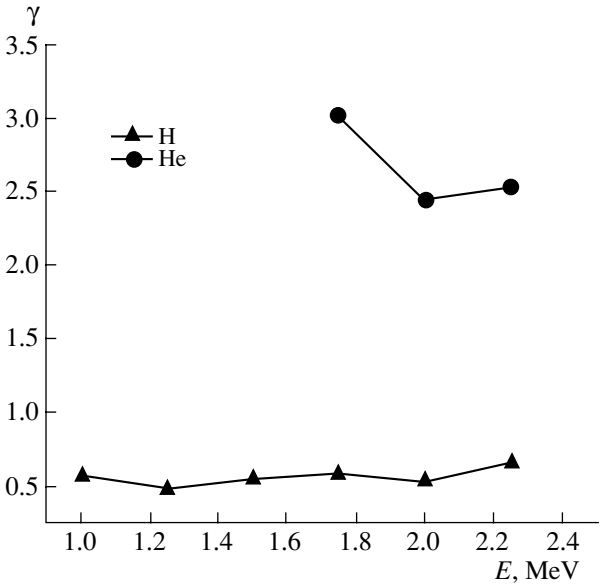

Fig. 12. Electron yield γ for a Sd/Cs cathode vs. energy of incident H^+ and He^+ ions.

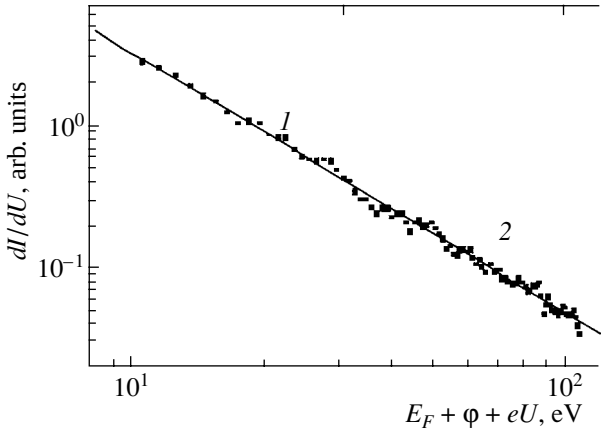

Fig. 13. Distribution function of the nonequilibrium electrons for GaAs bombarded with 1.25-MeV He^+ ions, plotted on a double logarithmic scale.

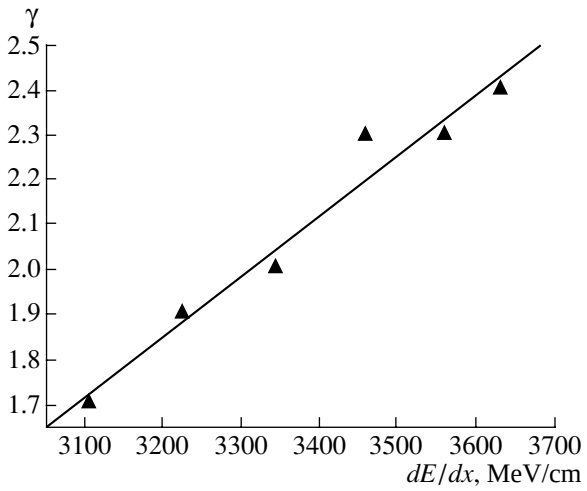

Fig. 14. Electron yield for germanium vs. specific ionization loss dE/dx for He^+ ions.

ductor plasma are power-law functions. Figure 13 shows (on a double logarithmic scale) a typical nonequilibrium EDF formed in a GaAs sample bombarded with 1.25-MeV He^+ ions. The experimental points can be well fit by a single straight line corresponding to the exponent $s = 2.9$ throughout the entire range of electron energies in vacuum (5–100 eV). Table 2 presents the exponents s obtained by processing the experimental data for all the samples under study and all the energies of the incident ions.

It was shown in our early experiments [20] that the EDFs formed in metal plasmas are piecewise power-law functions with different exponents in different energy ranges. At least two such ranges were revealed.

In our opinion, the piecewise power-law shape of the EDFs in experiments with metals, namely, the presence of two characteristic energy ranges, could be related to two different mechanisms for energy transfer from a fast incident ion to the electron subsystem of a solid. These mechanisms are (i) the excitation of collective plasma oscillations with a subsequent ionization in the electric field of these oscillations and (ii) inelastic collisions, resulting in the direct ionization of atoms. The energy of the electrons produced due to ionization via plasma oscillations cannot exceed the plasmon energy E_p in a substance. In semiconductors, the energy of plasmons related to conduction electrons is much lower than the ionization potential of atoms. For this reason, the distribution function in a semiconductor plasma is characterized by one power-law segment throughout the entire electron energy range under study.

The measurements of the energy spectrum of SIEE electrons have shown that, for all of the ion energies under study, the nonequilibrium EDFs formed in plasma are power-law in character.

As was mentioned above, the main integral characteristic of SIEE is the electron yield γ. Table 3 shows the yields of electron emission induced by He^+ ions for some semiconductors. It can be seen from Fig. 14 that, in germanium, the measured values of γ plotted versus the ionization loss dE/dx for He^+ ions are well fitted by a straight line; i.e., these quantities are indeed proportional to one another.

Table 2

Ion	Energy, MeV	Exponent s		
		GaAs	Ge	CdTe
He^+	1.00	–	2.8	–
	1.25	2.9	2.8	–
	1.50	2.9	2.8	–
	1.75	2.6	2.7	2.9
	2.00	2.6	2.8	2.8
	2.26	2.7	2.8	2.9
H^+	1.00	3.1	2.9	3.1
	1.25	2.9	2.8	3.0
	1.50	2.8	2.9	3.0
	1.75	2.8	2.6	2.7
	2.00	2.7	2.6	2.7
	2.26	3.0	2.8	2.8

Table 3

Energy, MeV	Electron yield γ		
	GaAs	Ge	CdTe
1.00	–	2.4	–
1.25	2.3	2.3	–
1.50	2.2	2.3	–
1.75	1.7	2.0	2.0
2.00	2.1	1.9	1.9
2.26	1.9	1.7	1.9

6. CONCLUSIONS

In this paper, we have shown that the presence of sources and sinks in a spatially uniform system leads to the formation of SNDs with power-law tails. A kinetic equation for the electrons scattered by acoustic phonons in a solid has been derived, and relations between power-law asymptotic solutions and the particle and energy fluxes in phase space have been established. The nonextensive thermodynamics of a nonequilibrium solid-state plasma has been developed based on the SNDs under study.

Numerical simulations of the formation of SNDs show that, for particles with Coulomb interaction, an SND is formed between the source and sink. Starting from a certain intensity of the source (sink), the power-law distribution function has the same exponent; i.e., it is universal. A radical change in the EEDF under nonequilibrium conditions leads to an anomalous increase in the conductivity and emissivity of the substance.

The experimental data on the EEDFs formed in the solid-state plasma of a Sb/Cs cathode irradiated with a beam of fast low-Z ions are presented. In all of the experiments with H^+ and He^+ ions, the nonequilibrium EEDFs in the energy range from 5 to 100 eV are found to have a piecewise power-law shape with different exponents in the energy ranges of 5–30 and 30–100 eV. The power exponents are expected to depend on the energy (specific ionization loss) of fast ions, and this was indeed observed for protons in the former energy range.

Our experimental studies of the formation of nonequilibrium electron distributions in a semiconductor plasma exposed to ion beams have shown that EEDFs have power-law asymptotes with one exponent. This is related to the low energy of the plasma oscillations carried by the conduction electrons.

ACKNOWLEDGMENTS

We are grateful to Prof. S.S. Moiseev (deceased), who initiated this study, for his continuous interest in this work. We are also grateful to the personnel of the VG-5 accelerator at the Kharkov Institute for Science and Technology and especially to V.M. Mishchenko for creating optimal conditions for our work. This study was supported by the Science and Technology Center in Ukraine, project no. 1862.

REFERENCES

1. A. V. Kats, V. M. Kontorovich, S. S. Moiseev, and V. E. Novikov, Preprint No. 42 (Institute of Radioelectronics, Academy of Sciences of the Ukr. SSR, Kharkov, 1974).
2. A. V. Kats, V. M. Kontorovich, S. S. Moiseev, and V. E. Novikov, Pis'ma Zh. Éksp. Teor. Fiz. **21**, 13 (1975) [JETP Lett. **21**, 5 (1975)]; Zh. Éksp. Teor. Fiz. **71**, 177 (1976) [Sov. Phys. JETP **44**, 93 (1976)].
3. V. I. Karas', S. S. Moiseev, and V. E. Novikov, Pis'ma Zh. Éksp. Teor. Fiz. **21**, 525 (1975) [JETP Lett. **21**, 245 (1975)]; V. I. Karas', Pis'ma Zh. Tekh. Fiz. **1** (21), 1020 (1975) [Sov. Tech. Phys. Lett. **1**, 438 (1975)].
4. V. I. Karas', S. S. Moiseev, and V. E. Novikov, Zh. Éksp. Teor. Fiz. **71**, 1421 (1976) [Sov. Phys. JETP **44**, 744 (1976)].
5. E. N. Batrakin, I. I. Zalyubovskiĭ, V. I. Karas', *et al.*, Zh. Éksp. Teor. Fiz. **89**, 1098 (1985) [Sov. Phys. JETP **62**, 633 (1985)].
6. E. N. Batrakin, I. I. Zalyubovskiĭ, V. I. Karas', *et al.*, Poverkhnost, No. 12, 82 (1986).
7. V. I. Karas', S. I. Kononenko, and V. I. Muratov, Vopr. At. Nauki Tekh., Ser.: Yad. Fiz. Issled. **1**, 71 (2001).
8. V. E. Novikov, A. V. Tur, and V. V. Yanovskiĭ, *Problems of Theoretical Physics* (Naukova Dumka, Kiev, 1986).
9. V. E. Novikov, S. S. Moiseev, and V. P. Seminozhenko, Fiz. Tekh. Poluprovodn. (Leningrad) **14**, 402 (1980) [Sov. Phys. Semicond. **14**, 236 (1980)].
10. V. I. Karas', V. E. Novikov, S. S. Moiseev, and V. P. Seminozhenko, Fiz. Nizk. Temp. **36**, 695 (1977) [Sov. J. Low Temp. Phys. **36**, 336 (1977)].
11. A. V. Bobylev, Dokl. Akad. Nauk SSSR **225**, 1041 (1975) [Sov. Phys. Dokl. **20**, 820 (1975)].
12. V. E. Novikov, S. S. Moiseev, *et al.*, Radiofiz. Radioastron. **4**, 160 (1999).
13. M. H. Ernst, in *Nonequilibrium Phenomena: I. The Boltzmann Equation*, Ed. by E. W. Montroll and J. L. Lebowitz (North-Holland, Amsterdam, 1983; Mir, Moscow, 1986), p. 51.
14. D. Petrina and A. Mishchenko, Dokl. Akad. Nauk SSSR **298**, 338 (1988) [Sov. Phys. Dokl. **33**, 32 (1988)].
15. V. E. Novikov, S. S. Moiseev, A. V. Tur, and V. V. Yanovskiĭ, Zh. Éksp. Teor. Fiz. **86**, 920 (1984) [Sov. Phys. JETP **59**, 537 (1984)].
16. F. G. Bass and Yu. G. Gurevich, *Hot Electrons and High-Power Electromagnetic Waves in Semiconductor Plasmas and Gas Discharges* (Nauka, Moscow, 1975).
17. C. Tsallis, J. Stat. Phys. **52**, 479 (1988); Braz. J. Phys. **29**, 1 (1999).
18. V. I. Karas' and V. E. Novikov, Vopr. At. Nauki Tekh., Ser.: Plazm. Élektron. Novye Metody Uskoreniya **4**, 157 (2003).
19. A. V. Bobylev, I. F. Potapenko, and V. A. Chuyanov, Zh. Vychisl. Mat. Mat. Fiz. **20**, 993 (1980).

20. V. M. Balebanov, V. I. Karas', I. V. Karas', *et al.*, Fiz. Plazmy **24**, 789 (1998) [Plasma Phys. Rep. **24**, 732 (1998)].
21. B. A. Trubnikov, in *Reviews of Plasma Physics*, Ed. by M. A. Leontovich (Gosatomizdat, Moscow, 1963; Consultants Bureau, New York, 1966), Vol. 1.
22. V. P. Silin, *Introduction to the Kinetic Theory of Gas* (Nauka, Moscow, 1971).
23. V. I. Karas' and I. F. Potapenko, Fiz. Plazmy **28**, 908 (2002) [Plasma Phys. Rep. **28**, 837 (2002)].
24. I. F. Potapenko, A. V. Bobylev, C. A. Azevedo, and A. S. Assis, Phys. Rev. E **56**, 7159 (1997).
25. I. F. Potapenko and V. A. Chuyanov, Zh. Vychisl. Mat. Mat. Fiz. **19**, 458 (1979).
26. A. S. Asseevskaya, E. B. Ivkin, and B. G. Kolomiets, Pis'ma Zh. Tekh. Fiz. **2**, 116 (1976) [Sov. Tech. Phys. Lett. **2**, 44 (1976)].
27. S. I. Anisimov, Ya. A. Imas, G. S. Romanov, and Yu. V. Khodyko, *The Effect of High-Power Radiation on Metals* (Nauka, Moscow, 1970).
28. N. P. Kalashnikov, V. S. Remizovich, and M. I. Ryazanov, *Collisions of Fast Charged Particles in Solids* (Atomizdat, Moscow, 1980).
29. V. P. Zhurenko, S. I. Kononenko, V. I. Karas', and V. I. Muratov, Fiz. Plazmy **29**, 150 (2003) [Plasma Phys. Rep. **29**, 130 (2003)].
30. Yu. V. Gott, *Particle Interaction with Substance in Plasma Studies* (Atomizdat, Moscow, 1978).
31. M. C. Steele and B. Vural, *Wave Interactions in Solid State Plasmas* (McGraw-Hill, New York, 1969; Atomizdat, Moscow, 1973).
32. E. J. Sternglass, Phys. Rev. **108**, 1 (1957).
33. H. Rothard, C. Caraby, A. Cassimi, *et al.*, Phys. Rev. A **51**, 3066 (1995).
34. B. A. Brusilovskiĭ, *Kinetic Ion–Electron Emission* (Énergoatomizdat, Moscow, 1990).
35. D. Hasselkamp, K. G. Lang, A. Scharmann, *et al.*, Nucl. Instrum. Methods Phys. Res. B **180**, 349 (1981).
36. J. Schou, Phys. Rev. B **22**, 2141 (1980).
37. W. Meckbach, G. Braunstein, and N. Arista, J. Phys. B **8**, L344 (1975).
38. D. Hasselkamp, S. Hippler, and A. Scharmann, Nucl. Instrum. Methods Phys. Res. B **18**, 561 (1987).
39. S. I. Kononenko, Dopovidi NANU, No. 1, 87 (2001).
40. V. I. Karas' and S. S. Moiseev, Ukr. Fiz. Zh. **24**, 1724 (1979).
41. V. M. Balebanov, S. S. Moiseev, V. I. Karas', *et al.*, At. Energ. **84**, 398 (1998).
42. N. A. Soboleva and A. E. Melamid, *Photoelectronic Devices* (Vysshaya Shkola, Moscow, 1974).
43. V. I. Karas', S. S. Moiseev, and A. P. Shuklin, Ukr. Fiz. Zh. **25**, 820 (1980).
44. V. S. Fomenko and I. A. Podchernyaeva, *Emission and Adsorption Properties of Substances and Materials* (Atomizdat, Moscow, 1975).

Translated by N.N. Ustinovskiĭ